

# BIOCHEMISTRY

© Copyright 2005 by the American Chemical Society

Volume 44, Number 50

December 20, 2005

## Articles

---

### Diversity of Function in the Isocitrate Lyase Enzyme Superfamily: The *Dianthus caryophyllus* Petal Death Protein Cleaves $\alpha$ -Keto and $\alpha$ -Hydroxycarboxylic Acids<sup>†</sup>

Zhibing Lu,<sup>‡</sup> Xiaohua Feng,<sup>‡</sup> Ling Song,<sup>‡</sup> Ying Han,<sup>‡</sup> Alexander Kim,<sup>‡</sup> Osnat Herzberg,<sup>§</sup> William R. Woodson,<sup>||</sup> Brian M. Martin,<sup>⊥</sup> Patrick S. Mariano,<sup>‡</sup> and Debra Dunaway-Mariano<sup>\*‡</sup>

Department of Chemistry, University of New Mexico, Albuquerque, New Mexico 87131, Center for Advanced Research in Biotechnology, University of Maryland Biotechnology Institute, Rockville, Maryland 20850, Department of Horticulture, Purdue University, West Lafayette, Indiana 47907, and Molecular Structure Unit Laboratory of Neurotoxicology, National Institute of Mental Health, National Institutes of Health, Bethesda, Maryland 20892

Received September 2, 2005; Revised Manuscript Received October 27, 2005

**ABSTRACT:** The work described in this paper was carried out to define the chemical function a new member of the isocitrate lyase enzyme family derived from the flowering plant *Dianthus caryophyllus*. This protein (Swiss-Prot entry Q05957) is synthesized in the senescent flower petals and is named the “petal death protein” or “PDP”. On the basis of an analysis of the structural contexts of sequence markers common to the C–C bond lyases of the isocitrate lyase/phosphoenolpyruvate mutase superfamily, a substrate screen that employed a (2*R*)-malate core structure was designed. Accordingly, stereochemically defined C(2)- and C(3)-substituted malates were synthesized and tested as substrates for PDP-catalyzed cleavage of the C(2)–C(3) bond. The screen identified (2*R*)-ethyl, (3*S*)-methylmalate, and oxaloacetate [likely to bind as the hydrate, C(2)(OH)<sub>2</sub> gem-diol] as the most active substrates (for each,  $k_{\text{cat}}/K_{\text{m}} = 2 \times 10^4 \text{ M}^{-1} \text{ s}^{-1}$ ). In contrast to the stringent substrate specificities previously observed for the *Escherichia coli* isocitrate and 2-methylisocitrate lyases, the PDP tolerated hydrogen, methyl, and to a much lesser extent acetate substituents at the C(3) position (*S* configuration only) and hydroxyl, methyl, ethyl, propyl, and to a much lesser extent isobutyl substituents at C(2) (*R* configuration only). It is hypothesized that PDP functions in oxalate production in Ca<sup>2+</sup> sequestering and/or in carbon scavenging from  $\alpha$ -hydroxycarboxylate catabolites during the biochemical transition accompanying petal senescence.

The work described in this paper was carried out to define the chemical function of an unknown protein in the isocitrate

<sup>†</sup> This work was supported by NIH Grants GM28688 (D.D.-M.) and MCB0235122 (O.H.) and by the Intramural Research Program of the NIH, NIMH (B.M.B.).

\* To whom correspondence should be addressed: Department of Chemistry, University of New Mexico, Albuquerque, NM 87131. Telephone: (505) 277-3383. Fax: (505) 277-6202. E-mail: dd39@unm.edu.

<sup>‡</sup> University of New Mexico.

<sup>§</sup> University of Maryland Biotechnology Institute.

<sup>||</sup> Purdue University.

<sup>⊥</sup> National Institutes of Health.

lyase (ICL<sup>1</sup>)/phosphoenolpyruvate mutase (PEPM) enzyme superfamily. This protein, hereafter called the petal death protein (PDP) (316 amino acids; Swiss-Prot entry Q05957), was discovered through the sequencing of a cDNA transcript prepared from mRNA synthesized in carnation flower petals (*Dianthus caryophyllus*) undergoing ethylene-induced senescence (1) [i.e., programmed cell death (2)]. The ICL/PEPM enzyme superfamily is presently known to consist of PEP mutase (3–8), phosphoenolpyruvate hydrolase (Ppyr hydrolase) (9), carboxyPEP mutase (CPEP mutase) (10, 11), 3-methyl-2-oxobutanoate hydroxymethyltransferase (MOBL)

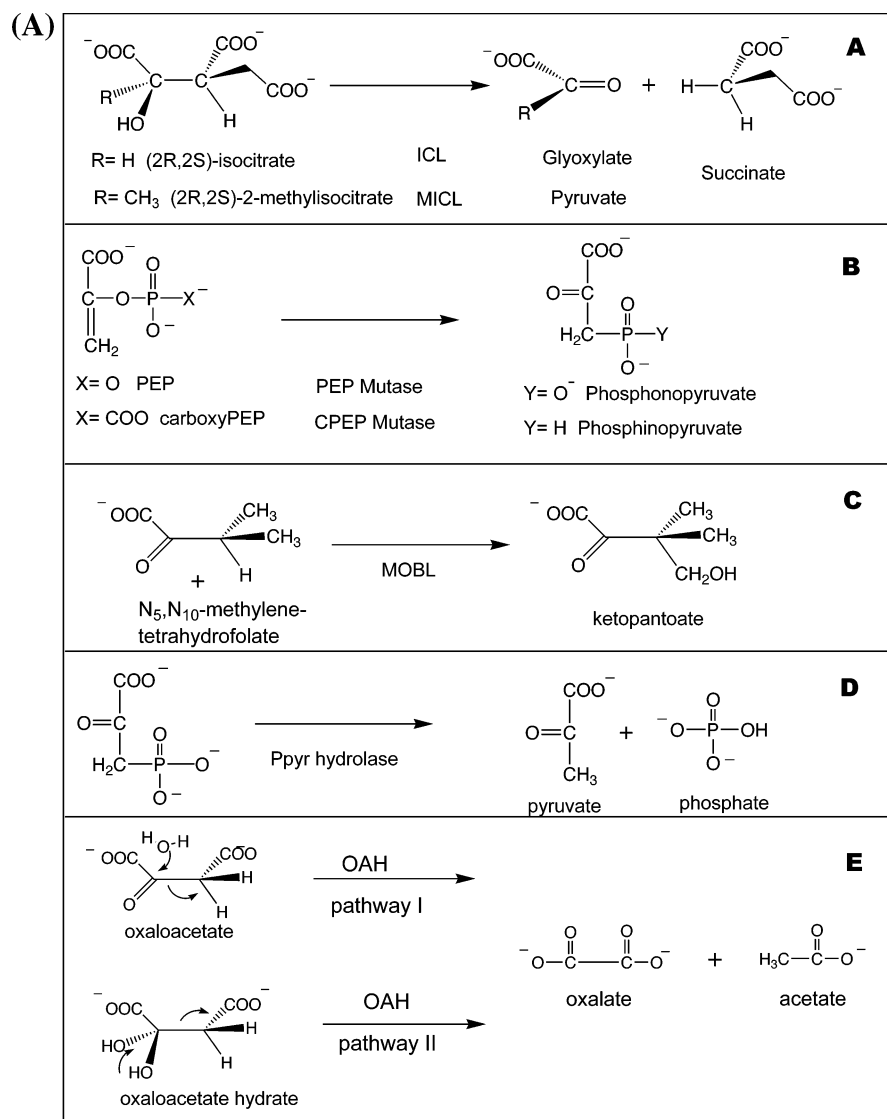
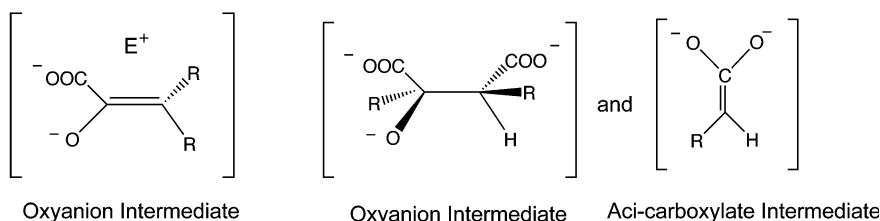
**(B) Mutase and Transferase****Lyase**

FIGURE 1: (A) Reactions catalyzed by known members of the isocitrate lyase superfamily. (A) The lyases ICL (isocitrate lyase) and MICL (2-methylisocitrate lyase). (B) The mutases PEP mutase (phosphoenolpyruvate mutase) and CPEP mutase (carboxyphosphoenolpyruvate). (C) The transferase MOB (3-methyl-2-oxobutanoate hydroxymethyltransferase). (D) The hydrolase Ppyr hydrolase (phosphonopyruvate hydrolase). (E) The putative lyase (pathway I) and hydrolase (pathway II) pathways of OAH (oxaloacetate hydrolase) catalysis. (B) Oxyanion reaction intermediates that are presumed to be stabilized by the mutase/transferase and lyase branches of the ICL/PEPM superfamily. E<sup>+</sup> represents the electrophile, which in the case of PEP mutase is metaphosphate and in the case of the 3-methyl-2-oxobutanoate hydroxymethyltransferase is N<sub>5</sub>, N<sub>10</sub>-methylene tetrahydrofolate.

(12–15), oxaloacetate hydrolase (OAH) (16, 17), isocitrate lyase (ICL) (18–22), and 2-methylisocitrate lyase (MICL) (23–27). The reactions catalyzed by these enzymes are illustrated in Figure 1A. The core chemistry of this superfamily is the stabilization of an oxyanion intermediate (and/or transition states). ICL, MICL, and OAH form a tetrahedral oxyanion intermediate in conjunction with an aci-carboxylate intermediate, whereas the PEP and CPEP mutases, Ppyr

hydrolase, and MOB form an enolate oxyanion as an intermediate (see Figure 1B).

The catalytic scaffold of the ICL/PEPM superfamily is formed at the C-terminal edge of an  $\alpha/\beta$ -barrel by nine peptide segments, one of which is derived from a swapped C-terminal  $\alpha$ -helix of an adjacent subunit [Figure 2A shows the catalytic scaffold in *Escherichia coli* 2-methylisocitrate lyase (27)]. The other eight peptide segments are derived

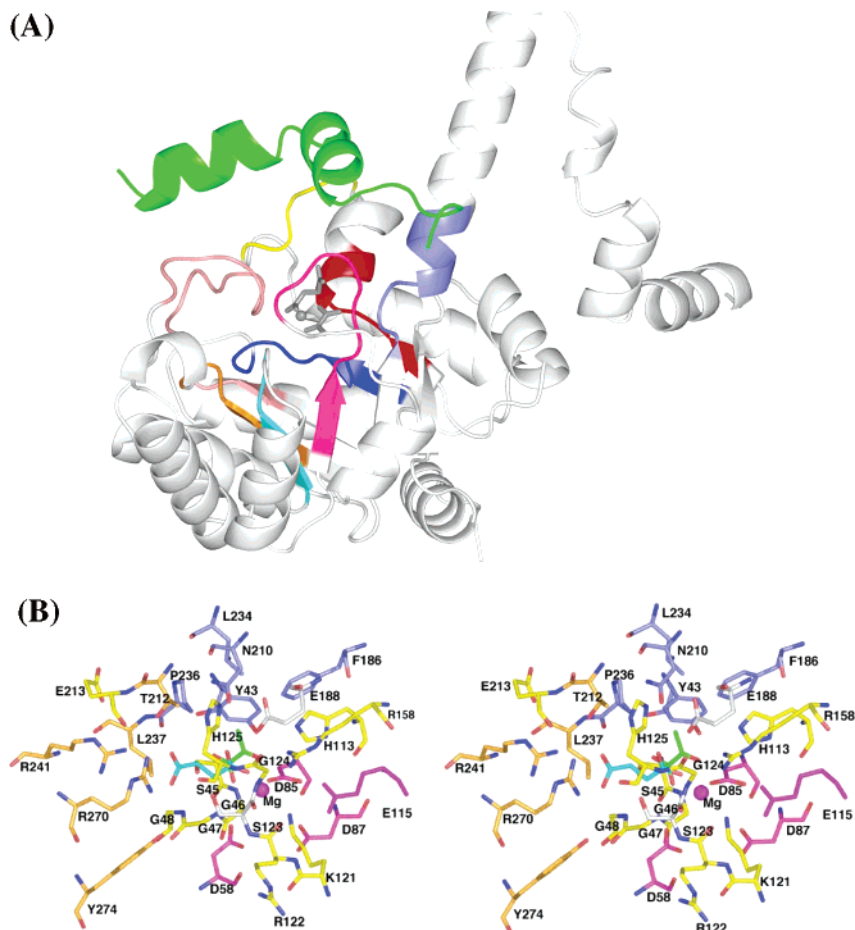


FIGURE 2: (A) Structure of the *E. coli* C123S 2-methylisocitrate lyase mutant bound with Mg<sup>2+</sup> (gray) and the product ligands pyruvate (gray) and succinate (gray). The backbone structure of subunit A of the homotetramer was drawn using the coordinates reported in ref 37 (Protein Data Bank entry 1xg3) using PyMol release 0.98 (DeLano Scientific LLC) to illustrate the nine protein segments (1–9) forming the catalytic scaffold. The amino acid sequences of these regions are listed in Figure 3 for 2-methylisocitrate lyase and the other known members of the ICL/PEPM superfamily. The color scheme and residue numbers are as follows: segment 1 (red, residues 43–49), segment 2 (yellow, residues 55–59), segment 3 (blue, residues 83–89), segment 4 (pink, residues 114–129), segment 5 (orange, residues 156–161), segment 6 (cyan, residues 184–188), segment 7 (magenta, residues 209–217), segment 8 (slate, residues 232–242), and segment 9 (green, subunit B residues 264\*–293\*). (B) Stereoview of the residues located within 5 Å of either product ligand. The nitrogen atoms are colored blue, the oxygen atoms colored red, and the carbon atoms color coded to indicate function. The Mg<sup>2+</sup> is colored magenta as are the carbon atoms of its four binding residues. The carbon atoms of the pyruvate ligand are colored green, and those of the succinate ligand are colored cyan. The catalytic Cys123 (mutated to Ser123 in the crystal structure) is colored gray as is the catalytic Glu188 [in its protonated form it donates a hydrogen bond to the substrate C(4)OO group]. The carbon atoms of the side chains that encase the (2*R*,3*S*)-2-methylisocitrate C(3)CH<sub>2</sub>COO substituent are colored brown, and those that encase the C(2)CH<sub>3</sub> group are colored slate. All other carbon atoms are colored yellow. Gly46 of segment 1 is located at the N-terminus of a nonbarrel helix. Its backbone amide, together with the backbone amide of the ensuing residue, provides an oxyanion hole to the substrate C(1) carboxylate group. Asp58 of segment 2 and the two Asp residues of segment 3 (positions 85 and 87) bind (directly or via bridging water molecules) the Mg<sup>2+</sup> cofactor that coordinates the substrate α-C(=O)COO unit. Arg158 of segment 5 engages in H-bond formation with the substrate α-C=O group. Segment 4 includes part of a flexible loop that gates the active site (17, 30–32, 37) and part of the preceding β-strand. The stringently conserved Glu-Asp...Lys motif (Figure 3) plays a key role in configuring the loop, and Glu115 binds the metal ion water ligand.

from the C-terminal regions of the β-strands, the loops connecting the α- and β-elements of the barrel, and the N-terminus of a nonbarrel helix. The first eight signature

segments are numbered sequentially starting with the N-terminus, and segment 9 is assigned to a C-terminal region of the adjacent subunit that traverses the top of the active site (6). The catalytic scaffold positions core residues and diversification residues, which are illustrated for 2-methylisocitrate lyase in Figure 2B. With the exception of the most divergent member, MOBL (14, 15), the core residues are stringently conserved among the family members (see the sequence alignment in Figure 3) as they serve to bind the common substrate α-C(=O)COO unit or the Mg<sup>2+</sup> cofactor. The diversification residues are used in the tailoring of the active site for a specific substrate and reaction type. Importantly, sequence alignments showed that PDP contains two key diversification residues (a Glu on segment 6 and a

<sup>1</sup> Abbreviations: PDP, petal death protein; ICL, isocitrate lyase; MICL, 2-methylisocitrate lyase; OAH, oxaloacetate hydrolase; MOBL, 3-methyl-2-oxobutanoate hydroxymethyltransferase; CPEP mutase, carboxyphosphoenolpyruvate mutase; PEP mutase, phosphoenolpyruvate mutase; Ppyr hydrolase, phosphoenolpyruvate hydrolase; LDH, lactate dehydrogenase; MDH, malate dehydrogenase; NADH, dihydronicotinamide adenine dinucleotide; K<sup>+</sup>Hepes, potassium salt of 4-(2-hydroxyethyl)-1-piperazineethanesulfonic acid; K<sup>+</sup>Mes, potassium salt of 2-(*N*-morpholino)ethanesulfonic acid; K<sup>+</sup>Pipes, potassium salt of piperazine-1,4-bis(2-ethanesulfonic acid); K<sup>+</sup>Taps, potassium salt of *N*-tris(hydroxymethyl)methyl-3-aminopropanesulfonic acid; K<sup>+</sup>Caps, potassium salt of *N*-cyclohexyl-3-aminopropanesulfonic acid; Capso, 3-(cyclohexylamino)-2-hydroxypropane.

	LOOP 1	LOOP 2	LOOP 3	LOOP 4	*
PEP mutase	W G S <b>G</b> L A <sup>49</sup>	G V R <b>D</b> S N <sup>60</sup>	L L <b>D</b> A <b>D</b> T G <sup>89</sup>	C L <b>E</b> D K L F P---K T N S L H D <sup>126</sup>	
P-pyr hydrolase	W G S <b>G</b> F E <sup>45</sup>	A V F <b>D</b> A N <sup>56</sup>	I A <b>D</b> I <b>D</b> T G <sup>85</sup>	V M <b>E</b> D K T F P---K D T S L R T <sup>122</sup>	
CPEP mutase	H M T <b>G</b> S G <sup>47</sup>	G L F <b>D</b> L G <sup>59</sup>	I M <b>D</b> A <b>D</b> A G <sup>88</sup>	H L <b>E</b> D Q V N P---K R C G H L E <sup>125</sup>	
ICL	Y L S <b>G</b> W Q <sup>94</sup>	T Y F <b>D</b> Q S <sup>110</sup>	V A <b>D</b> G <b>E</b> A G <sup>157</sup>	H W <b>E</b> D Q L A S E K K C G H L G <sup>195</sup>	
MICL	Y L S <b>G</b> G G <sup>47</sup>	G L F <b>D</b> L G <sup>59</sup>	L V <b>D</b> A <b>D</b> I G <sup>88</sup>	H I <b>E</b> D Q V G A---K R C G H R P <sup>126</sup>	
PDP	F V S <b>G</b> Y S <sup>69</sup>	G L F <b>D</b> F G <sup>81</sup>	V V <b>D</b> A <b>D</b> T G <sup>111</sup>	F L <b>E</b> D Q V W P---K K C G H M R <sup>148</sup>	
OAH	Y M T <b>G</b> A G <sup>68</sup>	G M A <b>D</b> L G <sup>80</sup>	I A <b>D</b> M <b>D</b> T G <sup>111</sup>	H I <b>E</b> D Q I Q N---K R C G H L Q <sup>148</sup>	

	LOOP 5	LOOP 6	LOOP 7	LOOP 8	LOOP 9
PEP mutase	V A <b>R</b> V E A <sup>162</sup>	I L M H S K <sup>192</sup>	I V P T K Y Y K <sup>221</sup>	V I W A N H N L R <sup>243</sup>	V S V K E I F R <sup>277</sup>
P-pyr hydrolase	I A <b>R</b> V E A <sup>158</sup>	I L I H S R <sup>188</sup>	L V P T A Y P Q <sup>217</sup>	V I Y G N H A I R <sup>240</sup>	P S V K E I I E <sup>274</sup>
CPEP mutase	I A <b>R</b> T D A <sup>159</sup>	I F L E A M <sup>188</sup>	A N M V E G G K <sup>214</sup>	A I Y P L S G W M <sup>239</sup>	M S F A E L F E <sup>276</sup>
ICL	I A <b>R</b> T D A <sup>231</sup>	I W M E T G <sup>287</sup>	Y N C S P S F N <sup>319</sup>	Q F I T L A G F H <sup>352</sup>	V E L Q E R E F <sup>381</sup>
MICL	M A <b>R</b> T D A <sup>160</sup>	L F P E A I <sup>189</sup>	A N I T E F G A <sup>215</sup>	A L Y P L S A F R <sup>240</sup>	M Q T R N E L Y <sup>273</sup>
PDP	V A <b>R</b> T D A <sup>182</sup>	T F V E A P <sup>211</sup>	A N M I E G G K <sup>237</sup>	I A H S L T A V Y <sup>262</sup>	M A T F S E F N <sup>295</sup>
OAH	I A <b>R</b> T D A <sup>184</sup>	G L L E G Y <sup>213</sup>	L N M V E N G S <sup>240</sup>	M I F S F A A L A <sup>265</sup>	N L T P K A L F <sup>296</sup>

FIGURE 3: Amino acid sequences of the nine peptide segments defining the catalytic scaffolds of ICL/PEPM superfamily members PEP mutase (*Mytilus edulis*), P-pyr hydrolase (phosphonopyruvate hydrolase from *Variovorax* sp.), CPEP mutase (carboxyPEP mutase from *Streptomyces hygroscopicus*), ICL (isocitrate lyase from *Mycobacterium tuberculosis*), MICL (2-methylisocitrate lyase from *E. coli*), PDP (petal death protein PSR132 from *D. caryophyllus*), and OAH (oxaloacetate hydrolase from *B. fückeliana*). The core residues are boxed, and the key diversification residues (Glu and Cys) that underlie isocitrate lyase and 2-methylisocitrate activities are marked with symbols.

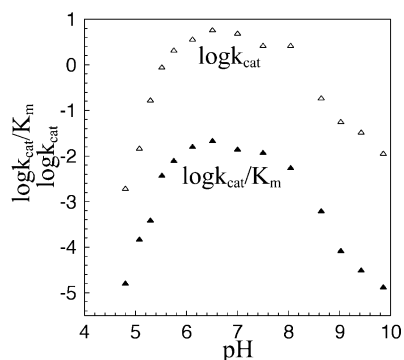


FIGURE 4: pH-rate profiles for the PDP-catalyzed reaction of (2R)-ethyl-(3S)-methyl malate measured in the presence of 5 mM MgCl<sub>2</sub> at 25 °C. See Materials and Methods for details.

Cys on segment 4) conserved in the CPEP mutase and in ICL, MICL, and OAH for acid-base catalysis (see Figure 3 and ref 27). The residues that encase the C(2) and C(3) substituents of the malate backbone of the isocitrate and 2-methylisocitrate are largely concentrated on segments 7–9. In MICL, the C(2)CH<sub>3</sub> group is surrounded by Tyr43 (segment 1), Phe186 (segment 6), Asn210 (segment 7), Leu234 (segment 8), and Pro236 (segment 8) and the C(3)-CH<sub>2</sub>COO group is surrounded by Thr212 (segment 7), Leu237 (segment 8), Arg241 (segment 8), Arg270\* (subunit B, segment 9), and Tyr274\* (subunit B, segment 9) (Figure 2B). These segments appear to play an especially important role in substrate specificity (see ref 27). The presence of the segment 4 motif K(K,R)C\*GH and segment 6 Glu in the PDP sequence suggests that it too is a lyase, but, as indicated by the sequence usage on segments 7–9 (Figure 3), one with a different substrate specificity.

Accordingly, a substrate screen for PDP function assignment was developed on the basis of the carbon scaffolds of malate (the backbone of isocitrate) and its oxidized form, oxaloacetate. In this paper, we report the results of this screen which demonstrate significant levels of catalytic activity toward C(2)–C(3) bond cleavage in oxaloacetate and in (2R)-alkylmalates and discuss the physiological role that these

activities might play in plant senescence. In the following paper (28), the X-ray structure of carnation PDP, which was ultimately determined, is presented and the mechanism of substrate recognition and catalysis is analyzed within this structural context.

## MATERIALS AND METHODS

**General.** Except where mentioned, all chemicals were purchased from Sigma-Aldrich. Custom-synthesized PCR primers were obtained from Invitrogen as were the restriction enzymes, the *pfu* polymerase, and the T4 DNA ligase. NMR spectra were recorded on a Bruker Avance 500 NMR instrument. DNA sequencing analysis was carried by the DNA Sequencing Facility of the University of New Mexico. SDS-PAGE was performed with gels prepared from a 12% acrylamide gel with a 3% stacking gel (37.5:1 acrylamide:biacrylamide ratio) (Bio-Rad). Mass spectrometry measurements of organic compounds were taken by the Mass Spectrometry Lab in the Department of Chemistry and Biochemistry of University of Maryland (College Park, MD). Optical rotation was measured with a model DIP-1000 Jasco polarimeter. *E. coli* isocitrate lyase and 2-methylisocitrate lyase were prepared as described previously (27). Protein concentrations were determined using the Bradford method (29).

**Cloning, Expression, and Purification.** The gene (GenBank accession number Q05957) encoding the PDP protein of *D. caryophyllus* (carnation flower) was amplified by PCR (30) from the PSR132 cDNA (1) using *pfuTurbo* DNA polymerase (Stratagene) and oligonucleotide primers with *Nde*I and *Bam*HI restriction sites, and cloned into the pET-3a vector (Novagen). The recombinant plasmid, PSR132-pET3a, was used to transform the *E. coli* BL21(DE3) plysS competent cells (Novagen). The cells were grown at 28 °C in Luria broth (LB) for 10 h to an OD<sub>600</sub> of ~1 in the presence of 50 µg/mL carbenicillin and then induced with 0.4 mM IPTG for 5 h at 30 °C. The cells were harvested by centrifugation, suspended in the lysis buffer [50 mM K<sup>+</sup>-Hepes (pH 7.5), 1 mM EDTA, 1 mM benzamide hydro-

chloride, 0.05 mg/mL trypsin inhibitor, 1 mM 1,10-phenanthroline, 0.1 mM PMSF, and 5 mM DTT], and passed through a French press. The cell lysate was centrifuged, and the supernatant was loaded onto a DEAE-cellulose column equilibrated with buffer A [50 mM triethanolamine (pH 7.5), 5 mM MgCl<sub>2</sub>, and 0.5 mM DTT] at 4 °C. The protein was eluted with a linear gradient of 0 to 0.3 M KCl in buffer A. The fractions containing PDP were supplemented with ammonium sulfate to 20% saturation and loaded onto a Phenyl-Sepharose column. The protein was eluted with a linear gradient of 20 to 0% saturated ammonium sulfate in buffer A, dialyzed against buffer A, and loaded onto a DEAE-Sepharose column. The protein was eluted with a linear gradient of 0 to 0.3 M KCl in buffer A and concentrated to 15 mg/mL using an Amicon cell. The protein, judged to be homogeneous on the basis of SDS-PAGE, was obtained in a yield of 7 mg/g of wet cells. The molar extinction coefficient at 280 nm, based on the Bradford protein determination, is 25 863 M<sup>-1</sup> cm<sup>-1</sup>. The purified protein was stored at -80 °C.

**PDP N-Terminal Sequence Determination.** PDP was chromatographed on a SDS-PAGE gel and transferred to a PVDF membrane (Novex Co.) and subjected to automated N-terminal amino acid sequencing to obtain the sequence PNGTTNGETEVEV.

**PDP Molecular Size Determination.** The theoretical MW of the recombinant PDP enzyme was calculated using the ExPASy Compute pI/MW tool (31). The subunit size of recombinant PDP enzyme was determined using SDS-PAGE in conjunction with molecular weight standards from Invitrogen. The subunit mass was determined TOF MS-ES mass spectrometry (University of New Mexico Mass Spectrometry Lab). The native molecular mass was determined with a Sephacryl S-200 gel filtration column (1.5 cm × 180 cm; Pharmacia) chromatography carried out at 4 °C using 0.1 M KCl with buffer B [50 mM K<sup>+</sup>Hepes and 0.5 mM DTT (pH 7.5)] as the eluant. The column was calibrated using a Pharmacia gel filtration calibration kit [thyroglobulin (669 000), catalase (232 000), albumin (67 000), and chymotrypsinogen A (25 000)].

**Site-Directed Mutants.** Site-directed mutagenesis was carried out using a PCR-based strategy (30) with *pfu* polymerase. Plasmid pET-3a-PSR132 was used as the template DNA for all the primary PCRs. Mutant protein purifications followed the same protocol as described for the wild-type recombinant enzyme.

**Reactants.** 3-Hydroxy-3-methylglutaric acid, oxaloacetate, citric acid, (*R*)-malic acid, (*S*)-malic acid, (*2R*)-methylmalic acid, (*2S*)-methylmalic acid, (*2R,3S*)-isocitric acid, and (*2S,3S:2R,3R*)-tartaric acid were purchased from Sigma-Aldrich. *threo*-(*2R,3S:2S,3R*)-2-methylisocitrate and *erythro*-(*2S,3S:2R,3R*)-2-methylcitrate were each prepared according to a published procedure (32) as was phosphonopyruvate (33). CarboxyPEP was provided by J. Gerlt (University of Illinois, Urbana, IL). (*2R,3S*)-Isopropylmalate (synthesized by M. Jung) and 3-butylmalate (Aldrich Rare Chemicals, catalog no. S789046) were provided by S. Clarke (University of California, Los Angeles, CA).

**Enzymatic Synthesis of (*2R,3S*)-2,3-Dimethylmalic Acid.** A 300 mL solution of 29 μM PDP, 5 mM MgCl<sub>2</sub>, 5 mM DTT, 500 mM sodium propionate, 500 mM sodium pyruvate, and 100 mM Tris buffer (pH 7.5) was stirred at 25 °C for 3

days. The solution was then diluted with 1 M KOH to a pH of ca. 10, and hydrogen peroxide (30% aqueous, 30 mL) was slowly added. The resulting solution was stirred at 90 °C for 30 min, and then 10 mg of catalase was added. The mixture was filtered through a 10 kDa membrane (Amicon), concentrated in vacuo to ca. 100 mL, adjusted with 12 M HCl to a pH of 1, and extracted with ethyl acetate. The ethyl acetate solution was dried over Na<sub>2</sub>SO<sub>4</sub> and concentrated in vacuo to yield a residue which was crystallized from ethyl acetate and petroleum ether, yielding 2.0 g of (*2R,3S*)-2,3-dimethylmalic acid: mp 99–100 °C [lit. (34–36) 99–100 and 97–99 °C]; [α]<sub>D</sub><sup>20</sup> -15.9 (*c* = 0.1, H<sub>2</sub>O) [lit. (34) -16.4 (*c* = 5, H<sub>2</sub>O)]; <sup>1</sup>H NMR (500 MHz, *d*<sub>3</sub>-acetone) δ 2.97 (q, *J* = 7.3 Hz, 1H), 1.34 (s, 3H), 1.26 (d, *J* = 7.3 Hz, 3H); <sup>13</sup>C NMR δ 177.2, 176.0, 74.9, 46.2, 23.6, 11.1; MS (*M* + 1) *m/z* 163.0615, calcd for C<sub>6</sub>H<sub>10</sub>O<sub>5</sub> *m/z* 163.0606.

**Enzymatic Synthesis (*2R*)-2-Ethylmalic Acid.** A 1 L solution of 10 μM PDP, 5 mM MgCl<sub>2</sub>, 1 mM DTT, 350 mM sodium acetate, 250 mM 2-ketobutyric acid, and 20 mM K<sup>+</sup>Hepes at pH 7.5 and 25 °C was gently stirred for 3 days, and adjusted with 1 M KOH to a pH of ca. 10. Hydrogen peroxide (30% aqueous, 40 mL) was slowly added and the resulting solution stirred at 100 °C for 60 min, filtered through a 10 kDa membrane (Amicon), concentrated in vacuo to ca. 100 mL, adjusted with 12 M HCl to a pH of 1, and extracted with ethyl acetate. The ethyl acetate layers were dried over Na<sub>2</sub>SO<sub>4</sub> and concentrated in vacuo to yield (*2R*)-2-ethylmalic acid (1.93 g) as a white solid: mp 147–148 °C (from ethyl acetate) [lit. 147–148 °C]; [α]<sub>D</sub><sup>25</sup> -14.8 (*c* = 0.4, H<sub>2</sub>O) [lit. (37) [α]<sub>D</sub><sup>20</sup> -14.4 (*c* = 1.02, H<sub>2</sub>O)]; <sup>1</sup>H NMR (500 MHz, *d*<sub>3</sub>-acetone) δ 2.92 and 2.63 (AB quartet, *J* = 16.3 Hz, 2H), 1.72 (m, 2H), 0.89 (t, *J* = 7.4 Hz, 3H); <sup>13</sup>C NMR δ 176.0, 172.1, 75.4, 43.1, 32.6, 7.5; MS (*M* + 1) *m/z* 163.0598, calcd for C<sub>6</sub>H<sub>10</sub>O<sub>5</sub> *m/z* 163.0606. The spectroscopic data for this substance matched those previously reported for the title compound (38).

**Enzymatic Synthesis of (*2R,3S*)-2-Ethyl-3-methylmalic Acid.** A 400 mL solution of 10 μM PDP, 5 mM MgCl<sub>2</sub>, 1 mM DTT, 350 mM sodium propionate, 250 mM 2-ketobutyric acid, and 20 mM K<sup>+</sup>Hepes (pH adjusted to 7.5 by addition of KOH) was gently stirred at 25 °C for 3 days and adjusted with 1 M KOH to a pH of ca. 10. Hydrogen peroxide (30% aqueous, 16 mL) was slowly added, and the resulting solution was stirred at 100 °C for 20 min, filtered through a 10 kDa membrane (Amicon), concentrated in vacuo to ca. 40 mL, adjusted with 12 M HCl to a pH of 1, and extracted with ethyl acetate. The ethyl acetate layers were dried over Na<sub>2</sub>SO<sub>4</sub> and concentrated in vacuo to yield a residue which was subjected to silica gel column chromatography (3:1 hexane/acetone) to give (*2R,3S*)-2-ethyl-3-methylmalic acid (1.8 g, 18%): mp 80–81 °C; [α]<sub>D</sub><sup>25</sup> -15.2 (*c* = 0.08, CH<sub>3</sub>OH); <sup>1</sup>H NMR (500 MHz, *d*<sub>3</sub>-acetonitrile) δ 2.91 (q, *J* = 7.3 Hz, 1H), 1.68 (m, 1H), 1.59 (m, 1H), 1.16 (d, *J* = 7.3 Hz, 3H), 0.80 (t, *J* = 7.45 Hz, 3H); <sup>13</sup>C NMR δ 177.6, 78.8, 46.4, 30.1, 11.5, 8.2; HRMS (*M* + Na) *m/z* 199.0580, calcd for C<sub>7</sub>H<sub>12</sub>O<sub>5</sub>Na *m/z* 199.0582.

**Enzymatic Synthesis of (*2R,3S*)-2-Propyl-3-methylmalic Acid.** A 400 mL solution of 10 μM PDP, 5 mM MgCl<sub>2</sub>, 1 mM DTT, 350 mM sodium propionate, 250 mM 2-oxovaleric acid, and 20 mM K<sup>+</sup>Hepes (pH 7.5) was gently stirred at 25 °C for 3 days. The solution was adjusted with 1 M KOH to a pH of ca. 10, and hydrogen peroxide (30% water solution,

16 mL) was slowly added. The resulting solution was stirred at 100 °C for 20 min, filtered through a 10 kDa membrane (Amicon), concentrated in vacuo to ca. 40 mL, adjusted with 12 M HCl to a pH of 1, and extracted with ethyl acetate (5 × 50 mL). The ethyl acetate layers were dried over Na<sub>2</sub>SO<sub>4</sub> and concentrated in vacuo to yield a residue which was subjected to silica gel column chromatography (3:1 hexane/acetone) to give (2*R*,3*S*)-2-propyl-3-methylmalic acid (1.2 g, 11%, oil): [α]<sub>D</sub><sup>25</sup> -13.3 (*c* = 0.114, CH<sub>3</sub>OH); <sup>1</sup>H NMR (500 MHz, *d*<sub>3</sub>-acetonitrile) δ 2.97 (q, *J* = 7.3 Hz, 1H), 1.65 (m, 1H), 1.57 (m, 1H), 1.40 (m, 1H), 1.20 (d, *J* = 7.3 Hz, 3H), 1.13 (m, 1H), 0.89 (t, *J* = 7.3 Hz, 3H); <sup>13</sup>C NMR δ 177.6, 177.5, 78.6, 46.5, 39.4, 17.6, 14.5, 11.4; HRMS (*M* + *Na*) *m/z* 213.0736, calcd for C<sub>8</sub>H<sub>14</sub>O<sub>5</sub>Na *m/z* 213.0739.

**Enzymatic Synthesis of (2*R*,3*S*)-2-Isobutyl-3-methylmalic Acid.** A 400 mL solution of 10 μM PDP, 5 mM MgCl<sub>2</sub>, 1 mM DTT, 350 mM sodium propionate, 250 mM 4-methyl-2-oxopentanoic acid sodium salt, and 20 mM K<sup>+</sup>Hepes (pH 7.5, by addition of KOH) was gently stirred at 25 °C for 3 days, and then with 1 M KOH adjusted to a pH of ca. 10. Hydrogen peroxide (30% water solution, 16 mL) was slowly added, and the solution was stirred at 100 °C for 20 min, filtered through a 10 kDa membrane (Amicon), and concentrated in vacuo to ca. 40 mL. After being adjusted with 12 M HCl to a pH of 1, the solution was extracted with ethyl acetate (5 × 50 mL). The ethyl acetate layers were dried over Na<sub>2</sub>SO<sub>4</sub> and concentrated in vacuo to yield a residue which was subjected to silica gel column chromatography (3:1 hexane/acetone) to give (2*R*,3*S*)-2-isobutyl-3-methylmalic acid (0.2 g, 2%, oil): [α]<sub>D</sub><sup>25</sup> -14.6 (*c* = 0.08, CH<sub>3</sub>OH); <sup>1</sup>H NMR (500 MHz, *d*<sub>3</sub>-acetonitrile) δ 2.89 (q, *J* = 7.3 Hz, 1H), 1.63 (m, 1H), 1.55 (m, 2H), 1.18 (d, *J* = 7.3 Hz, 3H), 0.92 (d, *J* = 6.5 Hz, 3H), 0.84 (d, *J* = 6.5 Hz, 3H); <sup>13</sup>C NMR δ 177.4, 177.2, 78.6, 47.5, 45.4, 25.2, 24.3, 11.7; HRMS (*M* + *Na*) *m/z* 227.0895, calcd for C<sub>9</sub>H<sub>16</sub>O<sub>5</sub>Na *m/z* 227.0896.

**Assay for CarboxyPEP Mutase Activity.** The conversion of carboxyPEP to phosphopyruvate was tested using the malate dehydrogenase (MDH) and NADH assay reported in ref 11. The reaction solution (1 mL) initially contained 1 mM carboxyPEP, 5 mM MgCl<sub>2</sub>, 10 μM PDP, 2.5 units/mL malate dehydrogenase, and 0.2 mM NADH in 50 mM K<sup>+</sup>Hepes (pH 7.5 and 25 °C). The absorbance of the solution was monitored at 340 nm (Δε = 6200 M<sup>-1</sup> cm<sup>-1</sup>) over a 20 min period. The control reaction, which did not include PDP, was run in parallel. There was no significant decrease in the absorbance of the PDP-containing reaction mixture over that of the control reaction mixture.

**Assay for Citrate Lysis Activity.** The oxalacetate from citrate lysis was detected by reduction with NADH and MDH. The reaction solutions (1 mL) initially contained 1 mM citrate, 5 mM MgCl<sub>2</sub>, 10 μM PDP, 2.5 units/mL MDH, and 0.2 mM NADH in 50 mM K<sup>+</sup>Hepes (pH 7.5 and 25 °C). The absorbance of the solution was monitored at 340 nm (Δε = 6200 M<sup>-1</sup> cm<sup>-1</sup>) over a 20 min period. The control reaction, which did not include PDP, was run in parallel.

**Assays for PEP Mutase and PEP Hydrolase Activities.** PDP-catalyzed conversion of phosphopyruvate to PEP was tested using the pyruvate kinase (PK)/ADP and lactate dehydrogenase (LDH)/NADH coupling system to convert PEP to lactate with the coupled conversion of NADH to NAD. The reaction solution (1 mL) initially contained 1 mM

phosphopyruvate, 5 mM MgCl<sub>2</sub>, 10 μM PDP, 10 units/mL PK, 10 units/mL LDH, 1 mM ADP, and 0.2 mM NADH in 50 mM K<sup>+</sup>Hepes (pH 7.5 and 25 °C). The absorbance of the solution was monitored at 340 nm (Δε = 6200 M<sup>-1</sup> cm<sup>-1</sup>) over a 20 min period. The control reaction, which did not include PDP, was run in parallel. There was no significant decrease in the absorbance in the PDP-containing mixture over that of the control reaction mixture. PDP-catalyzed pyruvate formed by PEP hydrolysis was detected with NADH and LDH. The reaction solutions (1 mL) initially contained 1 mM PEP, 5 mM MgCl<sub>2</sub>, 10 μM PDP, 10 units/mL LDH, and 0.2 mM NADH in 50 mM K<sup>+</sup>Hepes (pH 7.5 and 25 °C). The absorbance of the solution was monitored at 340 nm (Δε = 6200 M<sup>-1</sup> cm<sup>-1</sup>) over a 20 min period. The control reaction, which did not include PDP, was run in parallel.

**Assay for Glyoxylate.** The glyoxylate formation from PDP-catalyzed lysis of (*R*)- and (*S*)-2-malate, 3-butylmalate (mixture of isomers), (2*R*,3*S*)-3-isopropylmalate, DL-tartaric acid, isocitrate, or 2-methylisocitrate was assayed using NADH and LDH. The reaction solutions (1 mL) initially contained 1 mM DL-tartaric acid or D-*s*-isocitrate, or *threo*-[(2*R*,3*S*),(2*S*,3*R*)]-2-methylisocitrate or *erythro*-[(2*S*,3*S*),(2*R*,3*R*)]-2-methylcitrate, and 5 mM MgCl<sub>2</sub>, 10 μM PDP, 10 units/mL LDH, and 0.2 mM NADH in 50 mM K<sup>+</sup>Hepes (pH 7.5 and 25 °C). The absorbance of the solution was monitored at 340 nm (Δε = 6200 M<sup>-1</sup> cm<sup>-1</sup>) over a 20 min period. The control reaction, which did not include PDP, was run in parallel.

**Assay for β-Oxobutyric Acid.** Formation of the β-oxobutyric acid from 3-hydroxy-3-methylglutaric acid was monitored with NADH and β-ketobutyric acid dehydrogenase. The reaction solutions (1 mL) initially contained 1 mM 3-hydroxy-3-methylglutaric acid, 5 mM MgCl<sub>2</sub>, 10 μM PDP, 10 units/mL β-ketobutyric acid dehydrogenase, and 0.2 mM NADH in 50 mM K<sup>+</sup>Hepes (pH 7.5 and 25 °C). The absorbance of the solution was monitored at 340 nm (Δε = 6200 M<sup>-1</sup> cm<sup>-1</sup>) over a 20 min period. The control reaction, which did not include PDP, was run in parallel.

**Assay for Malate Substrates. (1) Continuous Assay.** The PDP activities with malate, 2,3-dimethyl malate, and 2-ethyl-3-methyl malate were measured at 25 °C using NADH and LDH. The reaction solutions (1 mL) initially contained 1 mM malate substrate, 5 mM MgCl<sub>2</sub>, 10 μM PDP, 10 units/mL LDH, and 0.2 mM NADH in 50 mM K<sup>+</sup>Hepes (pH 7.5 and 25 °C). The absorbance of the solution was monitored at 340 nm (Δε = 6200 M<sup>-1</sup> cm<sup>-1</sup>) over a 20 min time period. Control reactions not including PDP were run in parallel.

**(2) Fixed-Time Assay.** After standing for fixed time periods (<20% conversion), 200 μL aliquots of solutions [2 mL, 50 mM K<sup>+</sup>Hepes (pH 7.5) and 5 mM MgCl<sub>2</sub>] containing 2 μM PDP and 20–300 μM 2,3-dimethylmalate, 0.13 μM PDP and 100–2000 μM 2-ethyl-3-methyl malate, 0.20 μM PDP and 60–1500 μM 2-*n*-propyl-3-methyl malate, or 3.99 μM PDP and 0.5–10 mM 2-isobutyl-3-methyl malate were quenched with 200 μL of 0.6 N HCl. A 100 μL aliquot of 0.4 M phenylhydrazine hydrochloride was added to the reaction solutions, and the resulting mixtures were stirred for 8 min and subjected to UV absorbance measurements at either 322 nm (for 2,3-dimethyl malate), 325 nm (2-ethyl-3-methyl malate), 325 nm (2-propyl-3-methyl malate), or 326 nm (2-isobutyl-3-methyl malate). The standard curve of each α-keto

acid hydrazone was constructed by using the same conditions employed in the enzyme reaction. The molar extinction coefficients for the hydrazones at the wavelength specified above were determined to be  $6.4 \text{ mM}^{-1} \text{ cm}^{-1}$  for pyruvic acid,  $6.3 \text{ mM}^{-1} \text{ cm}^{-1}$  for  $\alpha$ -ketobutyric acid,  $7.4 \text{ mM}^{-1} \text{ cm}^{-1}$  2-oxovaleric acid, and  $6.7 \text{ mM}^{-1} \text{ cm}^{-1}$  for 4-methyl-2-oxopentanoic acid. The background absorbance of each corresponding malate reactant and propionate product was checked under the same condition as the enzyme reaction (mixed with  $200 \mu\text{L}$  of  $0.6 \text{ N HCl}$ , and then incubated with  $100 \mu\text{L}$  of  $0.4 \text{ M PH}$  for 8 min).

**Oxaloacetate Hydrolase Assay.** Oxaloacetate hydrolase activity was assayed according to a published procedure (16). Reaction solutions (1 mL) contained 5 mM  $\text{MgCl}_2$  or 0.3 mM  $\text{MnCl}_2$ ,  $0.22 \mu\text{M}$  PDP, and oxaloacetate (0.1–1.0 mM) in 0.1 M imidazole (pH 7.6 and  $25^\circ\text{C}$ ). The reaction was monitored at 255 nm for the disappearance of oxaloacetate ( $\epsilon = 1100 \text{ M}^{-1} \text{ cm}^{-1}$ ). The products formed from reaction of  $13 \mu\text{M}$  PDP with 30 mM oxaloacetate in 50 mM potassium phosphate containing 5 mM  $\text{MgCl}_2$  (pH 7 and  $25^\circ\text{C}$ ) were examined by  $^{13}\text{C}$  NMR. Following incubation for 2 h, the enzyme was removed using a centricon and  $\text{D}_2\text{O}$  was added to a final concentration of 20% (v/v) before the spectrum was measured with methanol serving as an internal standard (49 ppm). The acetate signals were apparent at 182.2 (COO) and 24.2 ppm ( $\text{CH}_3$ ).

**Steady-State Kinetic Constant Determination.** A PDP stock solution ( $\sim 30 \mu\text{M}$ ) was prepared in buffer A at pH 7.5. The steady-state kinetic parameters ( $K_m$  and  $k_{\text{cat}}$ ) for reactions catalyzed by PDP were determined from initial reaction velocities measured at varying substrate concentrations (ranging from  $0.5K_m$  to  $5K_m$ ). The data were fitted to eq 1 with KinetAsystI

$$V_o = V_{\text{max}}[S]/(K_m + [S]) \quad (1)$$

where  $V_o$  is the initial velocity,  $V_{\text{max}}$  is the maximum velocity,  $[S]$  is the substrate concentration, and  $K_m$  is the Michaelis–Menten constant for the substrate. The  $k_{\text{cat}}$  value was calculated from  $V_{\text{max}}$  and  $[E]$  according to the equation  $k_{\text{cat}} = V_{\text{max}}/[E]$ , where  $[E]$  is the protein subunit molar concentration in the reaction calculated from the ratio of measured protein concentration and the protein molecular mass (34 200 Da).

The competitive inhibition constant  $K_i$  was determined for phosphonopyruvate and oxalate by fitting initial velocity data to eq 2 with KinetAsystI

$$V_o = V_{\text{max}}[S]/[K_m(1 + [I]/K_i) + [S]] \quad (2)$$

Reaction solutions (1 mL) contained 200–2000  $\mu\text{M}$  (2*R*,3*S*)-dimethylmalate, 5 mM  $\text{MgCl}_2$ , 2  $\mu\text{M}$  PDP, 20–50  $\mu\text{M}$  phosphonopyruvate or oxalate, 0.2 mM NADH, 10 units/mL LDH, and 0.2 mM NADH in 50 mM  $\text{K}^+$ Hepes (pH 7.5 and  $25^\circ\text{C}$ ). The absorbance of the reaction solution was monitored at 340 nm.

**Metal Ion Activation of PDP.** The metal cofactor specificity was examined using (2*R*,3*S*)-2-ethyl-3-methyl malate as a substrate to produce 2-ketobutyrate and propionate as products. The 2-ketobutyrate was assessed using the LDH/NADH coupling system. The PDP was first dialyzed against 50 mM  $\text{K}^+$ Hepes (pH 7.5) buffer. Reaction solutions (1 mL)

contained  $\sim 0.5 \mu\text{M}$  PDP, 1 mM (2*R*,3*S*)-2-ethyl-3-methylmalic acid, 10 units/mL LDH, 0.2 mM NADH, and varying concentrations of  $\text{MgCl}_2$ ,  $\text{MnCl}_2$ ,  $\text{CoCl}_2$ ,  $\text{NiCl}_2$ , and  $\text{FeSO}_4$  or 1 mM  $\text{CaCl}_2$ ,  $\text{CuBr}_2$ , and  $\text{BaCl}_2$  in 50 mM  $\text{K}^+$ Hepes (pH 7.5 and  $25^\circ\text{C}$ ). The initial velocity data were analyzed using eq 1 and KinetAsystI.

**Determination of pH–Rate Profiles for PDP Catalysis.** The pH dependence of PDP catalysis was measured using (2*R*,3*S*)-2-ethyl-3-methyl malate as the substrate (0.2–3 mM), 5 mM  $\text{MgCl}_2$  as the cofactor, and 10 units/mL LDH and 0.2 mM NADH as the coupling system. The reaction solutions were buffered at pH 4.0–5.5 with 25 mM acetic acid and 25 mM Mes, pH 5.5–6.5 with 50 mM Mes, pH 6.5–7.0 with 50 mM Pipes, pH 7.0–8.0 with 50 mM Hepes, pH 8.0–8.5 with 50 mM Tricine, pH 8.5–9.0 with 50 mM Taps, pH 9.0–9.5 with 50 mM Capso, and pH 9.5–10.0 with 50 mM Caps. The initial velocity was fitted with eq 1 to obtain  $k_{\text{cat}}$  and  $k_{\text{cat}}/K_m$ , which in turn were used with eq 3 and KinetAsystI to calculate the  $\text{p}K_a$  values of the ionizing groups.

$$\log Y = \log(c/1 + [H]/K_1 + K_2/[H]) \quad (3)$$

where  $Y = k_{\text{cat}}$  or  $k_{\text{cat}}/K_m$ ,  $c$  is the pH-dependent value of  $Y$ ,  $[H]$  is the hydrogen ion concentration, and  $K_1$  and  $K_2$  are dissociation constants of groups that ionize.

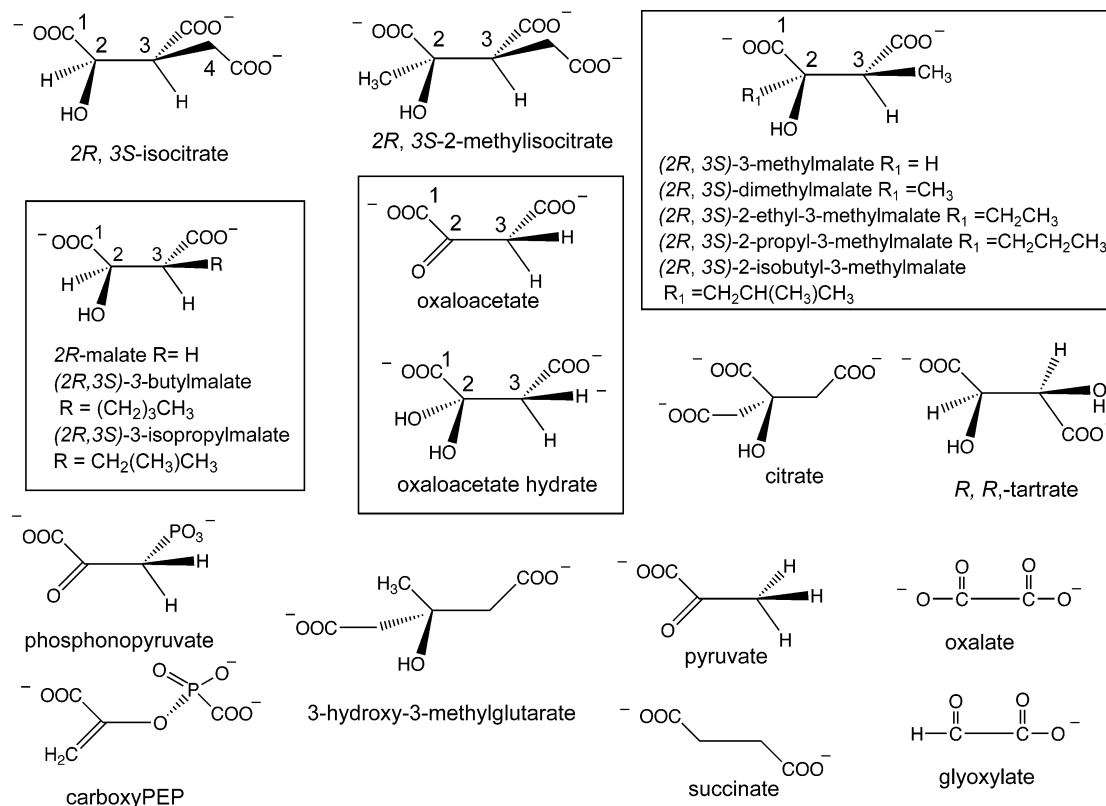
## RESULTS AND DISCUSSION

**PDP Preparation and Size Determination.** The recombinant *D. caryophyllus* PDP was purified to homogeneity in a yield of 7 mg/g of wet cells by using a column chromatography-based protocol. The theoretical mass of PDP is 34 180 Da, whereas that determined by mass spectral techniques is  $33\,879 \pm 4$  Da. The protein was subjected to N-terminal amino acid sequencing to yield the sequence PNGTT-NGETEV, which predicts a molecular mass of 33 880.5 Da for the isolated protein, consistent with the experimental value. Thus, the recombinant protein loses the first three encoded amino acids (MAP) during post-translational modification. The SDS–PAGE analysis gave an estimated subunit mass of 35 kDa, whereas the native mass measured using molecular size gel filtration chromatography was 133 kDa. Native PDP is therefore a homotetramer.

**PDP Catalytic Function Determination.** The first step taken in PDP function determination was to test the known activities of isocitrate lyase family members to confirm that PDP has a novel catalytic function.<sup>2</sup> To optimize activity detection, reaction mixtures containing high PDP (10  $\mu\text{M}$ ) and reactant (1 mM) concentrations in 50 mM  $\text{K}^+$ Hepes containing 5 mM  $\text{MgCl}_2$  (pH 7.5 and  $25^\circ\text{C}$ ) were incubated for an extended reaction period (reactant and product structures are shown in Chart 1 and Figure 1A). No PEP mutase (phosphonopyruvate to PEP) or carboxyPEP mutase (carboxyPEP to phosphinopyruvate) activities were observed within the detection limit of  $k_{\text{cat}} < 1 \times 10^{-5} \text{ s}^{-1}$ . Very low lyase activity ( $1 \times 10^{-4} \text{ s}^{-1}$ ) was observed with (2*R*,3*S*)-isocitrate and with the synthetic samples of (2*R*,3*S*)- and (2*S*,3*R*)-2-methylisocitrate and (2*R*,3*R*)- or (2*S*,3*S*)-2-methyl-

<sup>2</sup> The 3-methyl-2-oxobutanoate hydroxymethyltransferase activity was not tested because it is not compatible with the presence of the loop 4 K(K,R)C\*GH motif in PDP.

Chart 1: Structures of Substrates, Products, and Inhibitors Used for the PDP Function Assignment

Table 1: Steady-State Kinetic Constants for the C–C Bond Cleavage Reactions<sup>a</sup> Catalyzed by the PDP in 50 mM K<sup>+</sup>Hepes and 5 mM MgCl<sub>2</sub> (pH 7.5 and 25 °C)

reactant	$k_{\text{cat}}$ (s <sup>-1</sup> )	$K_m$ (μM)	$k_{\text{cat}}/K_m$ (M <sup>-1</sup> s <sup>-1</sup> )
(2R,3S)-isocitrate	$(1.3 \pm 0.1) \times 10^{-4}$	42 ± 2	3
(2R,3R:2S,3S)-2-methyl isocitrate	$(5.6 \pm 0.1) \times 10^{-4}$	104 ± 11	5
(2R,3S:2S,3R)-2-methyl isocitrate	$(1.4 \pm 0.1) \times 10^{-4}$	69 ± 1	2
oxaloacetate	2.72 ± 0.06	130 ± 10	2 × 10 <sup>4</sup>
(R)-malate or (S)-malate	< 1 × 10 <sup>-5</sup>		
(2R)-2-methyl malate	$(2.1 \pm 0.1) \times 10^{-1}$	290 ± 20	7 × 10 <sup>2</sup> <sup>b</sup>
(2S)-2-methyl malate	< 1 × 10 <sup>-5</sup>		
(2R)-2-ethyl malate	2.47 ± 0.05	1100 ± 100	2 × 10 <sup>3</sup> <sup>b</sup>
(2R,3S)-2,3-dimethyl malate	$(3.37 \pm 0.05) \times 10^{-2}$	26 ± 2	1 × 10 <sup>3</sup> <sup>b</sup>
	$(2.8 \pm 0.1) \times 10^{-2}$	29 ± 3	1 × 10 <sup>3</sup> <sup>c</sup>
(2R)-ethyl-(3S)-methyl malate	8.4 ± 0.1	530 ± 30	2 × 10 <sup>4</sup> <sup>b</sup>
	2.18 ± 0.08	450 ± 50	5 × 10 <sup>3</sup> <sup>c</sup>
(2R)-propyl-(3S)-methyl malate	$(2.81 \pm 0.04) \times 10^{-1}$	98 ± 5	3 × 10 <sup>3</sup> <sup>c</sup>
(2R)-isobutyl-(3S)-methyl malate	$(5.8 \pm 0.4) \times 10^{-1}$	8000 ± 500	7 × 10 <sup>1</sup> <sup>c</sup>

<sup>a</sup> The structures of the reactants and products are shown in Chart 1. <sup>b</sup> The kinetic constants were determined using the continuous LDH/NADH coupling assay. <sup>c</sup> The kinetic constants were determined using the fixed-time phenylhydrazine-based assay.

isocitrate (see Table 1). The products formed in these reactions are succinate and glyoxylate or pyruvate, respectively (Chart 1 and Figure 1A). In contrast, significant oxaloacetate hydrolase activity was evident. The product acetate was verified by <sup>13</sup>C NMR (see Materials and Methods), although the oxalate signal, which is intrinsically weak, could not be distinguished over the baseline noise. Initial velocity techniques were used to determine the steady-state kinetic constants for catalysis in 100 mM imidazole containing 5 mM MgCl<sub>2</sub> or 0.3 mM MnCl<sub>2</sub> (pH 7.6 and 25 °C). With 5 mM MgCl<sub>2</sub> serving as an activator,  $k_{\text{cat}} = 2.72 \pm 0.06 \text{ s}^{-1}$  and  $K_m = 130 \pm 10 \mu\text{M}$  ( $k_{\text{cat}}/K_m = 2.1 \times 10^4 \text{ M}^{-1} \text{ s}^{-1}$ ). With 0.3 mM MnCl<sub>2</sub> serving as an activator,  $k_{\text{cat}} = 37 \pm 1 \text{ s}^{-1}$  and  $K_m = 540 \pm 40 \mu\text{M}$  ( $k_{\text{cat}}/K_m = 7 \times 10^4 \text{ M}^{-1} \text{ s}^{-1}$ ). For comparison, the kinetic constants were

determined for recombinant *Botryotinia fuckeliana* oxaloacetate hydrolase<sup>3</sup> assessed using the same conditions that were used for the PDP-catalyzed reaction of oxaloacetate. With 5 mM MgCl<sub>2</sub> serving as an activator,  $k_{\text{cat}} = 15.5 \pm 0.2 \text{ s}^{-1}$  and  $K_m = 65 \pm 3 \mu\text{M}$  ( $k_{\text{cat}}/K_m = 2.4 \times 10^5 \text{ M}^{-1} \text{ s}^{-1}$ ), and with 0.3 mM MnCl<sub>2</sub> serving as an activator,  $k_{\text{cat}} = 45.7 \pm 0.9 \text{ s}^{-1}$  and  $K_m = 250 \pm 10 \mu\text{M}$  ( $k_{\text{cat}}/K_m = 2 \times 10^5 \text{ M}^{-1} \text{ s}^{-1}$ ). Overall, the efficiency of the PDP-catalyzed hydrolysis of oxaloacetate is within 1 order of magnitude of that of the fungal oxaloacetate hydrolase.

<sup>3</sup> The *B. fuckeliana* oxaloacetate hydrolase gene, which has been cloned for expression in *E. coli*, was provided to us by J. Henk-Jan and P. Schaap of Wageningen University (Wageningen, The Netherlands) for the purpose of substrate specificity and structure determination of the encoded enzyme.

The PDP-catalyzed oxaloacetate hydrolysis might occur by one of two pathways that are illustrated in Figure 1A for oxaloacetate hydrolase. According to pathway I, the enzyme active site binds and activates a water molecule for nucleophilic addition to the C(2)=O group of the oxaloacetate ligand. The oxyanion intermediate thus formed eliminates the acetate carbanion as the leaving group en route to product. For pathway II, the enzyme active site binds the C(2) gem-diol derived from solution hydration of oxaloacetate. The process of C(2)OH deprotonation and elimination of the acicarboxylate anion which ensues is identical to the pathway followed by the isocitrate and 2-methylisocitrate lyases (see the discussion in ref 27). At this point in time, we cannot distinguish between these two pathways. Previous  $^{13}\text{C}$  NMR studies have shown that oxaloacetate exists in aqueous solution as an equilibrium mixture of the ketone (C1 168.4 ppm, C2 200.7 ppm, C3 49.6 ppm, C4 175.6 ppm), enol (C3 98.9 ppm), and gem-diol (C2 94.5 ppm, C3 45.3 ppm) (39). By measuring the  $^{13}\text{C}$  NMR spectrum of 400 mM oxaloacetate in aqueous solution at pH 7.5, we showed that in the PDP reaction solution oxaloacetate exists as a mixture of ketone (C1 169.3 ppm, C2 201.3 ppm, C3 50.0 ppm, C4 175.4 ppm), enol (C3 99.0 ppm), and gem-diol (C2 94.8 ppm, C3 45.3 ppm). Thus, the ketone and the gem-diol are available for reaction with PDP in a roughly 13:1 ratio, and consequently either pathway is viable, although we tend to favor pathway II (gem-diol) as it is the standard lyase pathway (27) and certainly the one used by PDP in the cleavage of the C(2)-alkylmalate substrates (see below).

The substrate activities of the *R* and *S* isomers of malate were tested under reaction conditions that provide a detection limit of  $1 \times 10^{-5} \text{ s}^{-1}$  for the catalytic turnover rate. No activity was observed. Malate is essentially an analogue of the oxaloacetate hydrate wherein one of the two C(2)OH groups is replaced by a hydrogen atom. In contrast to the absence of substrate activity observed with the malate, (2*R*)-methyl malate [also known as (*R*)-citramalate] is converted to pyruvate and acetate with a  $k_{\text{cat}}$  of  $(2.1 \pm 0.1) \times 10^{-1} \text{ s}^{-1}$  and a  $K_{\text{m}}$  of  $290 \pm 20 \mu\text{M}$  ( $k_{\text{cat}}/K_{\text{m}} = 7 \times 10^2 \text{ M}^{-1} \text{ s}^{-1}$ ). The (2*S*)-2-methylmalate, on the other hand, is not a substrate. This result shows that the PDP, like the isocitrate and 2-methylisocitrate lyases, catalyzes cleavage of the C(2)–C(3) bond in (2*R*)-C(2)hydroxy carboxylate metabolites. This specificity is consistent with the architecture of the active site, and the conservation of the pocket of the (2*R*)-C(2)-hydroxy carboxylate (Figure 2B). The higher activity observed with the 2-methyl malate versus the 2-methyl isocitrate or isocitrate indicates that the binding pockets (segment 7 in particular, Figures 2 and 3) that accommodate the leaving group (acetate vs succinate) have diverged.

The observation that the (2*R*)-2-methylmalate is a viable substrate whereas (*R*)-malate is not indicates that a substituent is required at C(2) for productive substrate binding. This requirement is reminiscent of the stringent specificity of 2-methylisocitrate lyase for (2*R*,3*S*)-2-methyl isocitrate (25, 27). (2*R*,3*S*)-Isocitrate is an inhibitor and not a substrate for 2-methylisocitrate lyase (27). The X-ray structure of the lyase–isocitrate complex shows that without the C(2)methyl group to anchor the ligand, it is bound in a slightly different orientation which precludes catalysis (27).

Assuming that the PDP-catalyzed oxaloacetate hydrolysis occurs via pathway II, the 3-fold higher activity observed

for oxaloacetate ( $k_{\text{cat}}/K_{\text{m}} = 2 \times 10^4 \text{ M}^{-1} \text{ s}^{-1}$ ) versus that of (2*R*)-2-methyl malate ( $k_{\text{cat}}/K_{\text{m}} = 7 \times 10^2 \text{ M}^{-1} \text{ s}^{-1}$ ) suggests that the polar C(2)OH substituent is preferred over the nonpolar C(2)CH<sub>3</sub> substituent. If the fraction of oxaloacetate which exists in the hydrated form is taken into consideration, the theoretical  $k_{\text{cat}}/K_{\text{m}}$  for the oxaloacetate hydrate is  $2.6 \times 10^5 \text{ M}^{-1} \text{ s}^{-1}$ .

To test additional stereochemically pure malate analogues, it was necessary to synthesize them. This was accomplished using the PDP to catalyze the reverse, C–C bond forming reaction. Specifically, the 2-ethyl malate was formed from reaction of acetate and 2-ketobutyrate, 2-ethyl-3-methyl malate from propionate and 2-ketobutyrate, 2,3-dimethyl malate from propionate and pyruvate, 2-propyl-3-methyl malate from propionate and 2-oxovalerate, and 2-isobutyl 3-propionate from propionate and 4-methyl 2-oxo-pentanoate. In each case, a single stereoisomer was generated which was shown to be C(3)-*S* and/or C(2)-*R*. Using the pure products as substrates in the lyase direction, the steady-state kinetic constants were measured (Table 1). The substitution of the C(2)methyl group of the (2*R*)-2-methyl malate with an ethyl group increased the  $k_{\text{cat}} \sim 10$ -fold ( $2.47 \pm 0.1 \text{ s}^{-1}$ ) but at the same time increased the  $K_{\text{m}} \sim 4$ -fold such that the net increase in  $k_{\text{cat}}/K_{\text{m}}$  ( $2 \times 10^3 \text{ M}^{-1} \text{ s}^{-1}$ ) is only  $\sim 3$ -fold. The addition of a methyl group at C(3) of the (2*R*)-2-methyl malate decreased the  $k_{\text{cat}} \sim 5$ -fold and decreased the  $K_{\text{m}} \sim 10$ -fold. The most active substrate is (2*R*,3*S*)-2-ethyl-3-methyl malate. The  $k_{\text{cat}}/K_{\text{m}}$  ( $2 \times 10^4 \text{ M}^{-1} \text{ s}^{-1}$ ) value of this substrate is within a physiologically significant range, even though this compound is not a known metabolite. Propyl group substitution at C(2) decreases both  $k_{\text{cat}}$  and  $K_{\text{m}}$  with no gain in  $k_{\text{cat}}/K_{\text{m}}$  ( $3 \times 10^3 \text{ M}^{-1} \text{ s}^{-1}$ ). The isobutyl group decreases  $k_{\text{cat}}$  and increases  $K_{\text{m}}$ , resulting in a significant decrease in  $k_{\text{cat}}/K_{\text{m}}$  ( $7 \times 10^1 \text{ M}^{-1} \text{ s}^{-1}$ ).

(2*R*,3*S*)-3-Isopropyl malate and 3-butyl malate (mixture of stereoisomers) were not active substrates, nor were the metabolites 3-hydroxy-3-methyl glutarate, citrate, and (2*S*,3*S*:2*R*,3*R*)-tartrate. Oxalate and phosphonopyruvate were found to be competitive inhibitors versus (2*R*)-2-methyl malate with  $K_{\text{i}}$  values of  $4.3 \pm 0.3$  and  $25.2 \pm 0.8 \mu\text{M}$ , respectively.

*pH and Metal Cofactor Requirements for PDP Catalysis.* The members of the ICL superfamily are activated by divalent metal ions, and PDP is no exception. The steady-state kinetic constants for metal ion activation of the PDP were determined at a fixed saturating concentration of (2*R*,3*S*)-2-ethyl-3-methyl malate (1 mM) and varying metal ion concentrations in 50 mM K<sup>+</sup>Hepes (pH 7.5 and 25 °C). The  $k_{\text{cat}}$  values fall in a narrow range of 2–3 s<sup>-1</sup>, whereas the  $K_{\text{m}}$  values varied significantly:  $19 \pm 1 \mu\text{M}$  for Mg<sup>2+</sup>,  $0.70 \pm 0.03 \mu\text{M}$  for Mn<sup>2+</sup>,  $2.0 \pm 0.2 \mu\text{M}$  for Co<sup>2+</sup>, and  $6.1 \pm 0.5 \mu\text{M}$  for Fe<sup>2+</sup>. Given the cellular concentrations of these metal, it is likely that Mg<sup>2+</sup> is the physiological activator.

The substrate screens had been carried out at pH 7.5 assuming that PDP conformed to the neutral pH maximum observed for other ICL superfamily members. The  $k_{\text{cat}}$  and  $k_{\text{cat}}/K_{\text{m}}$  values were determined at varying concentrations of (2*R*,3*S*)-2-ethyl-3-methyl malate and 1 mM MgCl<sub>2</sub> as a function of the reaction solution pH to show that this assumption was nearly correct (pH 7.0 would be optimal). The profiles were bell-shaped and defined optimal catalytic functioning at or near neutral pH. The acid range of the log  $k_{\text{cat}}$  profile defines an essential base residue, which in the

protonated form ionizes with an apparent  $pK_a$  value of 4.5. The alkaline range of the  $\log k_{cat}$  profile defines an essential acid residue that ionizes with an apparent  $pK_a$  value of 9.3. The acid region of the  $\log k_{cat}/K_m$  profile defines an essential base residue that in the protonated form ionizes with apparent  $pK_a$  values of 5.3. The alkaline pH range of the  $\log k_{cat}/K_m$  profile defines an essential acid residue that ionizes with an apparent  $pK_a$  value of 9.0. No attempt has yet been made to assign these ionizations to active site residues.

**PDP Site-Directed Mutants Confirm the Function of Core Residue Asp79 and Lyase Diversification Residue Cys144.** The kinetic constants of D79A (segment 2, Figure 3) and C144A (segment 4, Figure 3) PDP site-directed mutants were measured at 25 °C using (2*R*,3*S*)-2-ethyl-3-methyl malate as a substrate and 1 mM MgCl<sub>2</sub> as an activator (K<sup>+</sup>Hepes, pH 7.5). The lyase activities of isocitrate lyase and 2-methylisocitrate lyase are dependent on the segment 4 Cys residue, believed to function in the protonation of the succinate aci-carboxylate anion intermediate (24, 27). By analogy, Cys144 of PDP might function in the protonation of the propionate carbanion intermediate generated by C(2)–C(3) bond cleavage in (2*R*,3*S*)-2-ethyl-3-methyl malate. As in the case of isocitrate lyase and 2-methylisocitrate lyase (18, 24), replacement of Cys144 of segment 4 with Ala in the PDP removes all detectable catalytic activity ( $k_{cat} < 1 \times 10^{-5} \text{ s}^{-1}$ ), consistent with its presumed role as general acid catalyst.

Asp79 is a core residue located on segment 2 whose role in the ICL/PEPM superfamily is to bind the Mg<sup>2+</sup> cofactor via the water ligand. It has been suggested that in the isocitrate and 2-methylisocitrate lyases, this Asp might participate in a proton relay in which the water ligand mediates the transfer of the proton from the substrate C(2)-OH (27). Replacement of Asp58 of segment 2 with Ala (equivalent to Asp79 in PDP) in 2-methylisocitrate lyase results in the loss of catalytic function (24). In PEP mutase, Asp58 of segment 2 binds a Mg<sup>2+</sup> water ligand and the side chain of Asn122 of segment 4 (5, 7, 8). This latter interaction is essential for PEP mutase active site desolvation. Replacement of Asp58 of PEP mutase with Ala precludes catalysis (7). In the PDP, the Ala for Asp79 replacement reduces the turnover rate 1000-fold:  $k_{cat} = (2.3 \pm 0.2) \times 10^{-3} \text{ s}^{-1}$  and  $K_m = 600 \pm 100 \mu\text{M}$ .

**PDP Physiological Function.** The PDP exhibits a unique but broad substrate profile compared to those of the other known ICL/PEPM superfamily lyases that each act strictly on a single substrate. PDP is similar to the isocitrate and 2-methylisocitrate lyases in that it catalyzes C(3)–C(2) bond cleavage within the (2*R*,3*S*)-malate framework, yet it has extremely low catalytic activity with (2*R*,3*S*)-isocitrate and (2*R*,3*S*)-2-methyl isocitrate. PDP is most active with (2*R*,3*S*)-malates that possess a methyl group at C(3) (as opposed to the CH<sub>2</sub>COO group characteristic of the isocitrate lyase and 2-methylisocitrate lyase substrates) and a small alkyl substituent at C(2). PDP also catalyzes the breakdown of oxaloacetate, the substrate active form of which is presumably the C(2) gem-diol (Figure 1, pathway II). However, PDP differs from the oxaloacetate hydrolase of the ICL family in that it is equally active with C(2)alkyl malates, while the *B. fückeliana* oxaloacetate hydrolase<sup>3</sup> examined in our lab exhibits only low activity toward malate derivatives (Y. Han and D. Dunaway-Mariano, unpublished data).

The other unique feature of the PDP is that whereas the  $k_{cat}/K_m$  values measured for *E. coli* isocitrate and 2-methylisocitrate lyases and the *B. fückeliana* oxaloacetate hydrolase with their physiological substrates are between  $1 \times 10^5$  and  $1 \times 10^6 \text{ M}^{-1} \text{ s}^{-1}$ , the  $k_{cat}/K_m$  values measured for PDP toward its two best substrates [oxaloacetate and (2*R*,3*S*)-2-ethyl-3-methyl malate] are only  $2 \times 10^4 \text{ M}^{-1} \text{ s}^{-1}$  ( $k_{cat}$  values of 2 and 8 s<sup>-1</sup>, respectively). The lower efficiency observed for the PDP is consistent with its broad substrate specificity, which suggests that the active site has not been optimized for binding a particular substrate structure. Nevertheless, the question of whether the “true” physiological substrate of PDP has been discovered remains. (2*R*)-2-Methyl malate (40–45) and (2*R*,3*S*)-2,3-dimethyl malate (46, 47) are known metabolites, and (2*R*)-2-methylmalate synthase (substrates being pyruvate and acetyl-CoA) and (2*R*,3*S*)-2,3-dimethylmalate lyase (products being pyruvate and propionate) are known enzymes. In addition, there is some evidence that ethyl and propyl malates are metabolites (48, 49). Thus, we might expect that 2-alkyl and 3-alkyl malates would be components of the plant metabolism. The PDP-catalyzed conversion of these compounds to smaller metabolites that feed into the citric acid cycle would thereby serve carbon recycling in senescent cells.

During senescence, flower petals export sugars and nitrogenous compounds which are produced by the degradation of polysaccharides, proteins, lipids, nucleic acids, and cell walls (50–56). The mRNA transcription profiling shows that many genes involved in this recycling effort are upregulated. Thus, one clue to PDP function is that it might be linked to the metabolism associated with carbon recovery from carnation petal cells. Indeed, the gene encoding ICL, a structural homologue of PDP, is among the genes that are heavily transcribed during programmed cell death in various plant tissues (57). ICL, which catalyzes the interconversion of isocitrate with succinate and glyoxalate (Figure 1A), is a key enzyme of the glyoxylate cycle. This cycle enables acetate derived from lipid breakdown to be converted to four-carbon gluconeogenic substrates and hence to sugars for export. Therefore, a possible connection exists between enhanced ICL synthesis and the metabolism associated with senescence. Our working hypothesis is that like ICL, PDP functions to catalyze C–C bond cleavage in one or more  $\alpha$ -hydroxy carbon acids derived from lipid or cell wall degradation.

The PDP-catalyzed conversion of oxaloacetate to acetate and oxalate might also play a role in plant senescence. Oxalate plays an important role in plants, sequestering and storing Ca<sup>2+</sup> (58). Accordingly, release of Ca<sup>2+</sup> in the dismantling cells might require enhanced oxalate production (P. Unkefer, personal communication).

The PDP was discovered through the sequencing of a cDNA transcript prepared from mRNA synthesized in carnation flower petals (*D. caryophyllus*) undergoing ethylene-induced senescence (1). An important question addressed at the outset of these studies is whether the carnation PDP function can be generalized to other plants. If the PDP is indeed essential to petal senescence, then the expectation is that paralogs of the carnation PDP exist in other flowering plants. Accordingly, the carnation PDP sequence was used as query in a Blast search of the *Arabidopsis thaliana* genome, presently the single representative of plant genomics

(59). As with *D. caryophyllus*, *A. thaliana* is a flowering plant that is subject to ethylene-induced programmed cell death (60). The search identified two genes located on chromosome I which encode nearly identical proteins whose sequences are 62% identical with that of the carnation PDP [GenBank accession numbers NP\_173565 (336 amino acids) and NP\_56148 (339 amino acids)]. On the basis of this high level of sequence identity, it is plausible that these *A. thaliana* proteins perform the same chemical catalysis as the carnation PDP. The *A. thaliana* genome encodes two other enzymes of the ICL/PEPM enzyme superfamily. First, on chromosome III, is the gene encoding the 576-amino acid ICL. This gene shares >70% sequence identity with other known ICLs but shares only 12% sequence identity with the carnation PDP; hence, it is a likely ICL. Second, located on chromosome II are four genes which encode isozymes that differ in their C-terminal sequence [GenBank accession numbers NP\_850388 (479 amino acids), NP\_973676 (478 amino acids), NP\_181847 (451 amino acids), and NP\_973677 (466 amino acids)] and which share 29% sequence identity with PDP. The lyase signature motif K(K,R)C\*GH of segment 4 (Figures 2 and 3) is not present in these isozymes, suggesting that they catalyze a novel reaction, different from that of the lyase clad.

## CONCLUSION

This work has shown that PDP is a carbon-carbon lyase that in plants targets (2*R*,3*S*)-malates, with preference for (2*R*,3*S*)-2-ethyl-3-methyl malate and oxaloacetate [as the C(2) gem-diol]. We speculate that PDP's relaxed substrate specificity contributes to its suggested role as a carbon scavenger. However, it is not clear whether this is by design or simply the characteristic of a poorly evolved enzyme catalyst functioning in a secondary metabolic process in which high specificity and optimal turnover rate are not essential. To gain insight into the structural basis of PDP substrate recognition and catalysis, the X-ray structure of PDP was determined. This structure is reported and analyzed with in the context of the structures of the other members of the ICL/PEPM superfamily in the following paper (28).

## ACKNOWLEDGMENT

We thank Dr. Wolfgang Buckel of Philipps University (Marburg, Germany) for providing us with a sample of synthetic *threo*-2-methyl isocitrate, Dr. John Gerlt of the Department of Biochemistry, University of Illinois, for a sample of synthetic carboxyphosphoenolpyruvate, and Dr. Steve Clarke and Mr. Darren Dumlao of the Department of Chemistry and Biochemistry, University of California, for samples of (2*R*,3*S*)-3-isopropyl malate and 3-butyl malate. Last, we thank Dr. Pat Unkefer of Los Alamos National Laboratories (Los Alamos, NM) for very helpful discussions of the genetics and the biochemistry of plant senescence.

## REFERENCES

- Wang, H., Brandt, A. S., and Woodson, W. R. (1993) A flower senescence-related mRNA from carnation encodes a novel protein related to enzymes involved in phosphonate biosynthesis, *Plant Mol. Biol.* 22, 719–24.
- van Doorn, W. G., and Woltering, E. J. (2005) Many ways to exit? Cell death categories in plants, *Trends Plant Sci.* 10, 117–22.
- Bowman, E., McQueney, M., Barry, R. J., and Dunaway-Mariano, D. (1988) Catalysis and thermodynamics of the phosphoenolpyruvate/phosphonopyruvate rearrangement. Entry into the phosphonate class of naturally occurring organophosphorus compounds, *J. Am. Chem. Soc.* 110, 5575–6.
- Seidel, H. M., Freeman, S., Seto, H., and Knowles, J. R. (1988) Phosphonate biosynthesis: Isolation of the enzyme responsible for the formation of a carbon-phosphorus bond, *Nature* 335, 457–8.
- Jia, Y., Lu, Z., Huang, K., Herzberg, O., and Dunaway-Mariano, D. (1999) Insight into the mechanism of phosphoenolpyruvate mutase catalysis derived from site-directed mutagenesis studies of active site residues, *Biochemistry* 38, 14165–73.
- Huang, K., Li, Z., Jia, Y., Dunaway-Mariano, D., and Herzberg, O. (1999) Helix swapping between two  $\alpha/\beta$  barrels: Crystal structure of phosphoenolpyruvate mutase with bound  $Mg^{2+}$ -oxalate, *Struct. Folding Des.* 7, 539–48.
- Liu, S., Lu, Z., Han, Y., Jia, Y., Howard, A., Dunaway-Mariano, D., and Herzberg, O. (2004) Conformational flexibility of PEP mutase, *Biochemistry* 43, 4447–53.
- Liu, S., Lu, Z., Jia, Y., Dunaway-Mariano, D., and Herzberg, O. (2002) Dissociative phosphoryl transfer in PEP mutase catalysis: Structure of the enzyme/sulfolpyruvate complex and kinetic properties of mutants, *Biochemistry* 41, 10270–6.
- Kulakova, A. N., Wisdom, G. B., Kulakov, L. A., and Quinn, J. P. (2003) The purification and characterization of phosphonopyruvate hydrolase, a novel carbon-phosphorus bond cleavage enzyme from *Variovorax* sp Pa12, *J. Biol. Chem.* 278, 23426–31.
- Hidaka, T., Seto, H., and Imai, S. (1989) Biosynthetic Mechanism of C-P Bond Formation: Isolation of Carboxyphosphoenolpyruvate and Its Conversion to Phosphinopyruvate, *J. Am. Chem. Soc.* 111, 8012–3.
- Pollack, S. J., Freeman, S., Pompliano, D. L., and Knowles, J. R. (1992) Cloning, overexpression and mechanistic studies of carboxyphosphoenolpyruvate mutase from *Streptomyces hygroscopicus*, *Eur. J. Biochem.* 209, 735–43.
- Jones, C. E., Brook, J. M., Buck, D., Abell, C., and Smith, A. G. (1993) Cloning and sequencing of the *Escherichia coli* panB gene, which encodes ketopantoate hydroxymethyltransferase, and overexpression of the enzyme, *J. Bacteriol.* 175, 2125–30.
- Sugantino, M., Zheng, R., Yu, M., and Blanchard, J. S. (2003) *Mycobacterium tuberculosis* ketopantoate hydroxymethyltransferase: Tetrahydrofolate-independent hydroxymethyltransferase and enolization reactions with  $\alpha$ -keto acids, *Biochemistry* 42, 191–9.
- Chaudhuri, B. N., Sawaya, M. R., Kim, C. Y., Waldo, G. S., Park, M. S., Terwilliger, T. C., and Yeates, T. O. (2003) The crystal structure of the first enzyme in the pantothenate biosynthetic pathway, ketopantoate hydroxymethyltransferase, from *M. tuberculosis*, *Structure* 11, 753–64.
- von Delft, F., Inoue, T., Saldanha, S. A., Ottenhof, H. H., Schmitzberger, F., Birch, L. M., Dhanaraj, V., Witty, M., Smith, A. G., Blundell, T. L., and Abell, C. (2003) Structure of *E. coli* ketopantoate hydroxymethyl transferase complexed with ketopantoate and  $Mg^{2+}$ , solved by locating 160 selenomethionine sites, *Structure* 11, 985–96.
- Lenz, H., Wunderwald, P., and Eggerer, H. (1976) Partial purification and some properties of oxalacetase from *Aspergillus niger*, *Eur. J. Biochem.* 65, 225–36.
- Ruijter, G. J., van de Vondervoort, P. J., and Visser, J. (1999) Oxalic acid production by *Aspergillus niger*: An oxalate-non-producing mutant produces citric acid at pH 5 and in the presence of manganese, *Microbiology* 145 (Part 9), 2569–76.
- Rehman, A., and McFadden, B. A. (1997) Cysteine 195 has a critical functional role in catalysis by isocitrate lyase from *Escherichia coli*, *Curr. Microbiol.* 35, 267–9.
- Vanni, P., Giachetti, E., Pinzauti, G., and McFadden, B. A. (1990) Comparative structure, function and regulation of isocitrate lyase, an important assimilatory enzyme, *Comp. Biochem. Physiol. B* 95, 431–58.
- Britton, K. L., Abeysinghe, I. S., Baker, P. J., Barynin, V., Diehl, P., Langridge, S. J., McFadden, B. A., Sedelnikova, S. E., Stillman, T. J., Weeradechapon, K., and Rice, D. W. (2001) The structure and domain organization of *Escherichia coli* isocitrate lyase, *Acta Crystallogr. D* 57, 1209–18.
- Britton, K., Langridge, S., Baker, P. J., Weeradechapon, K., Sedelnikova, S. E., De Lucas, J. R., Rice, D. W., and Turner, G.

- (2000) The crystal structure and active site location of isocitrate lyase from the fungus *Aspergillus nidulans*, *Struct. Folding Des.* 8, 349–62.
22. Sharma, V., Sharma, S., Hoener zu Bentrup, K., McKinney, J. D., Russell, D. G., Jacobs, W. R., Jr., and Sacchettini, J. C. (2000) Structure of isocitrate lyase, a persistence factor of *Mycobacterium tuberculosis*, *Nat. Struct. Biol.* 7, 663–8.
  23. Horswill, A. R., and Escalante-Semerena, J. C. (1999) *Salmonella typhimurium* LT2 catabolizes propionate via the 2-methylcitric acid cycle, *J. Bacteriol.* 181, 5615–23.
  24. Grimek, T. L., Holden, H., Rayment, I., and Escalante-Semerena, J. C. (2003) Residues C123 and D58 of the 2-methylisocitrate lyase (PrpB) enzyme of *Salmonella enterica* are essential for catalysis, *J. Bacteriol.* 185, 4837–43.
  25. Grimm, C., Evers, A., Brock, M., Maerker, C., Klebe, G., Buckel, W., and Reuter, K. (2003) Crystal structure of 2-methylisocitrate lyase (PrpB) from *Escherichia coli* and modelling of its ligand bound active centre, *J. Mol. Biol.* 328, 609–21.
  26. Simanshu, D. K., Satheskumar, P. S., Savithri, H. S., and Murthy, M. R. (2003) Crystal structure of *Salmonella typhimurium* 2-methylisocitrate lyase (PrpB) and its complex with pyruvate and Mg<sup>2+</sup>, *Biochem. Biophys. Res. Commun.* 311, 193–201.
  27. Liu, S., Lu, Z., Han, Y., Melamud, E., Dunaway-Mariano, D., and Herzberg, O. (2005) Crystal structures of 2-methylisocitrate lyase in complex with product and with isocitrate inhibitor provide insight into lyase substrate specificity, catalysis and evolution, *Biochemistry* 44, 2949–62.
  28. Teplyakov, A., Liu, S., Lu, Z., Howard, A., Dunaway-Mariano, D., and Herzberg, O. (2005) Crystal Structure of the Petal Death Protein from Carnation Flower, *Biochemistry* 44, 16377–16384.
  29. Bradford, M. M. (1976) A rapid and sensitive method for the quantitation of microgram quantities of protein utilizing the principle of protein-dye binding, *Anal. Biochem.* 72, 248–54.
  30. Erlich, H. A., Ed. (1992) *PCR Technology Principles and Applications for DNA Amplification*, W. H. Freeman and Co., New York.
  31. Appel, R. D., Bairoch, A., and Hochstrasser, D. F. (1994) A new generation of information retrieval tools for biologists: The example of the ExPASy WWW server, *Trends Biochem. Sci.* 19, 258–60.
  32. Brock, M., Darley, D., Textor, S., and Buckel, W. (2001) 2-Methylisocitrate lyases from the bacterium *Escherichia coli* and the filamentous fungus *Aspergillus nidulans*: Characterization and comparison of both enzymes, *Eur. J. Biochem.* 268, 3577–86.
  33. Anderson, V. E., Weiss, P. M., and Cleland, W. W. (1984) Reaction intermediate analogues for enolase, *Biochemistry* 23, 2779–86.
  34. Lill, U., Pirzer, P., Kukla, D., Huber, R., and Eggerer, H. (1980) Nicotinic acid metabolism enzymic preparation and absolute configuration of the substrate for 2,3-dimethylmalate lyase, *Hoppe Seyler's Z. Physiol. Chem.* 361, 875–84.
  35. Pirzer, P., Lill, U., and Eggerer, H. (1979) Nicotinic acid metabolism. 2,3-Dimethylmalate lyase, *Hoppe Seyler's Z. Physiol. Chem.* 360, 1693–702.
  36. Calderari, G., and Seebach, D. (1985) Asymmetric Michael-Additions. Stereoselective Alkylation of Chiral, Non-Racemic Enolates by Nitroolefins. Preparation of Enantiomerically Pure  $\gamma$ -Aminobutyric and Succinic Acid Derivatives, *Helv. Chim. Acta* 68, 1592–604.
  37. Palmisano, G., Dosi, I., Monti, D., and Pellegata, R. (1990) An Efficient Entry to Highly Functionalised C4 Chiral Synthons via Lewis Acid-Catalysed Ene Reaction of (1S)-Pinene and -Keto Esters. Part 4, *J. Chem. Soc., Perkin Trans. 1*, 1875–990.
  38. Spencer, H. K., Khatri, H. N., and Hil, R. K. (1976) Stereochemistry of some acetyl coenzyme A condensations, *Bioorg. Chem.* 5, 177–86.
  39. Buldain, G., De Los Santos, C., and Frydman, B. (1985) Carbon-13 nuclear magnetic resonance spectra of the hydrate, keto and enol forms of oxaloacetic acid, *Magn. Reson. Chem.* 23 (6), 478–81.
  40. Buckel, W., and Barker, H. A. (1974) Two pathways of glutamate fermentation by anaerobic bacteria, *J. Bacteriol.* 117, 1248–60.
  41. Kato, Y., and Asano, Y. (1997) 3-Methylaspartate ammonia-lyase as a marker enzyme of the mesaconate pathway for (S)-glutamate fermentation in Enterobacteriaceae, *Arch. Microbiol.* 168, 457–63.
  42. Howell, D. M., Xu, H., and White, R. H. (1999) (R)-Citramalate synthase in methanogenic archaea, *J. Bacteriol.* 181, 331–3.
  43. Herter, S., Fuchs, G., Bacher, A., and Eisenreich, W. (2002) A bicyclic autotrophic CO<sub>2</sub> fixation pathway in *Chloroflexus aurantiacus*, *J. Biol. Chem.* 277, 20277–83.
  44. Osumi, T., and Katsuki, H. (1977) A novel pathway for L-citramalate synthesis in *Rhodospirillum rubrum*, *J. Biochem.* 81, 771–8.
  45. Ivanovsky, R. N., Krasilnikova, E. N., and Berg, I. A. (1997) A Proposed Citramalate Cycle for Acetate Assimilation in the Purple Non-Sulfur Bacterium *Rhodospirillum rubrum*, *FEMS Microbiol. Lett.* 153, 399–404.
  46. Kollmann-Koch, A., and Eggerer, H. (1984) Nicotinic acid metabolism. Dimethylmaleate hydratase, *Hoppe Seyler's Z. Physiol. Chem.* 365, 847–57.
  47. Rabin, R., Salamon, I., Bleiweis, A. S., Carlin, J., and Ajl, S. J. (1968) Metabolism of ethylmalic acids by *Pseudomonas aeruginosa*, *Biochemistry* 7, 377–88.
  48. Imai, K., Reeves, H. C., and Ajl, S. J. (1963) N-Propylmalate Synthetase, *J. Biol. Chem.* 238, 3193–8.
  49. Rabin, R., Reeves, H. C., and Ajl, S. J. (1963)  $\beta$ -Ethylmalate Synthetase, *J. Bacteriol.* 86, 937–44.
  50. van Doorn, W. G., Balk, P. A., van Houwelingen, A. M., Hoebrechts, F. A., Hall, R. D., Vorst, O., van der Schoot, C., and van Wordragen, M. F. (2003) Gene expression during anthesis and senescence in Iris flowers, *Plant Mol. Biol.* 53, 845–63.
  51. van Doorn, W. G. (2004) Is petal senescence due to sugar starvation? *Plant Physiol.* 134, 35–42.
  52. Charlton, W. L., Johnson, B., Graham, I. A., and Baker, A. (2005) Non-coordinate expression of peroxisome biogenesis,  $\beta$ -oxidation and glyoxylate cycle genes in mature *Arabidopsis* plants, *Plant Cell Rep.* 23, 647–53.
  53. Buchanan-Wollaston, V., Earl, S., Harrison, E., Mathas, E., Navabpour, S., Page, T., and Pink, D. (2003) The molecular analysis of leaf senescence a genomics approach, *Plant Biotechnol. J.* 1, 3–22.
  54. Guo, Y., Cai, Z., and Gan, S. (2004) Transcriptome of *Arabidopsis* leaf senescence, *Plant Cell Environ.* 27, 521–49.
  55. Buchanan-Wollaston, V., Page, T., Harrison, E., Breeze, E., Lim, P. O., Nam, H. G., Lin, J. F., Wu, S. H., Swidzinski, J., Ishizaki, K., and Leaver, C. J. (2005) Comparative transcriptome analysis reveals significant differences in gene expression and signalling pathways between developmental and dark/starvation-induced senescence in *Arabidopsis*, *Plant J.* 42, 567–85.
  56. Hortensteiner, S., and Feller, U. (2002) Nitrogen metabolism and remobilization during senescence, *J. Exp. Bot.* 53, 927–37.
  57. Fargeix, C., Gindro, K., and Widmer, F. (2004) Soybean (*Glycine max.* L.) and bacteroid glyoxylate cycle activities during nodular senescence, *J. Plant Physiol.* 161, 183–90.
  58. Franceschi, V. R., and Nakata, P. A. (2005) Calcium Oxalate in Plants: Formation and Function, *Annu. Rev. Plant Biol.* 56, 41–71.
  59. Theologis, A., Ecker, J. R., Palm, C. J., Federspiel, N. A., Kaul, S., White, O., Alonso, J., Altafi, H., Araujo, R., Bowman, C. L., Brooks, S. Y., Buehler, E., Chan, A., Chao, Q., Chen, H., Cheuk, R. F., Chin, C. W., Chung, M. K., Conn, L., Conway, A. B., Conway, A. R., Creasy, T. H., Dewar, K., Dunn, P., Etgu, P., Feldblyum, T. V., Feng, J., Fong, B., Fujii, C. Y., Gill, J. E., Goldsmith, A. D., Haas, B., Hansen, N. F., Hughes, B., Huizar, L., Hunter, J. L., Jenkins, J., Johnson-Hopson, C., Khan, S., Khaykin, E., Kim, C. J., Koo, H. L., Kremenetskaia, I., Kurtz, D. B., Kwan, A., Lam, B., Langin-Hooper, S., Lee, A., Lee, J. M., Lenz, C. A., Li, J. H., Li, Y., Lin, X., Liu, S. X., Liu, Z. A., Luros, J. S., Maiti, R., Marziali, A., Militscher, J., Miranda, M., Nguyen, M., Nierman, W. C., Osborne, B. I., Pai, G., Peterson, J., Pham, P. K., Rizzo, M., Rooney, T., Rowley, D., Sakano, H., Salzberg, S. L., Schwartz, J. R., Shinn, P., Southwick, A. M., Sun, H., Tallon, L. J., Tambunga, G., Toriumi, M. J., Town, C. D., Utterback, T., Van Aken, S., Vaysberg, M., Vysotskaia, V. S., Walker, M., Wu, D., Yu, G., Fraser, C. M., Venter, J. C., and Davis, R. W. (2000) Sequence and analysis of chromosome 1 of the plant *Arabidopsis thaliana*, *Nature* 408, 816–20.
  60. Kieber, J. J. (1997) The ethylene response pathway in *Arabidopsis*, *Annu. Rev. Plant Physiol. Plant Mol. Biol.* 48, 277–96.